ELSEVIER

Journal of Fluorine Chemistry 110 (2001) 145–151

JOURNAL OF FLUORINE CHEMISTRY

www.elsevier.com/locate/jfluchem

Raman scattering study of highly fluorinated graphite

Vinay Gupta[a], Tsuyoshi Nakajima[a,*], Boris Žemva[b]

[a]*Department of Applied Chemistry, Aichi Institute of Technology, Yakusa-cho, Toyota-shi 470-0392, Japan*
[b]*Jožef Stefan Institute, Jamova 39, 1000 Ljubljana, Slovenia*

Received 28 November 2000; accepted 20 March 2001

Dedicated to late Dr. Karel Lutar

Abstract

Raman spectra of highly fluorinated C_xF samples ($1 < x < 2$) prepared at room temperature and 515°C were measured. C_xF samples prepared at room temperature exhibited two Raman bands at 1593–1583 and 1555–1542 cm^{-1}. Graphite samples fluorinated at 515°C for 1 and 2 min also gave similar bands at 1581–1580 and 1550–1538 cm^{-1}. However, graphite samples fluorinated from 15 min to 10 h at 515°C no longer showed such spectra. The Raman peaks shifted to lower frequencies with increasing fluorine concentration in C_xF. This trend is due to the weakening of the C–C bonds of the graphene layers. Observation of both kinds of Raman bands suggests the coexistence of two highly fluorinated phases, C_2F and C_1F, in the samples. The process of formation of graphite fluoride is discussed on the basis of the Raman spectra of C_xF samples obtained at 515°C.

Keywords: Raman spectra; Intercalation compound; Fluorinated graphite; Graphite fluoride

1. Introduction

Among many graphite intercalation compounds (GICs), the fluorine–graphite intercalation compound (C_xF) shows very peculiar behavior due to the special properties of elemental fluorine, namely its high reactivity and its low dissociation energy. Intercalation of fluorine into graphite would be difficult in "a pure fluorine atmosphere" at temperatures below ca. 100°C [1–18]. The reaction system consisting of graphite and elemental fluorine is usually contaminated by traces of HF. It is considered that the fluorine atom with its small polarizability and high electronegativity does not form a charge transfer complex with graphite in a pure fluorine atmosphere, but is covalently bonded to a carbon atom at the graphite edge [4,8,9,13–15]. Diffusion of fluorine into graphene layers is difficult under such conditions. However, in the presence of a small amount of a fluoride such as HF, AsF_5 or a light metal fluoride like LiF, fluorine forms a charge transfer complex with graphite at low temperatures, having a high diffusibility [1–18]. The C–F bonds remain nearly ionic for stage ≥ 2 with a single layer of intercalated fluorine atoms in the graphene layers. The electrical conductivity shows metallic behavior [3,4,8,9,13,19–25]. With the formation of stage 1 C_xF, C–F bonds change from nearly ionic to semi-ionic and intercalated fluorine atoms gradually form a double layer with close packing of atoms [1–18]. This leads to a sharp decrease in the electrical conductivity [13,21,22]. At higher temperatures, i.e. 350–600°C, elemental fluorine reacts with graphite yielding graphite fluorides, $(C_2F)_n$ and $(CF)_n$ which are black to white [3,26]. These graphite fluorides are electrical insulators. One of the objectives in our recent studies has been the synthesis of C_xF ($x < 2$) by a one-step fluorination reaction at room temperature. The synthesis and electrochemical behavior of such highly fluorinated graphite was recently reported [27].

Raman spectroscopy is a powerful tool for studying the phonon characteristics of GICs of both donor and acceptor type [28]. In particular, the stage dependence of Raman-active E_{2g2} mode frequencies reveals that charge density in the graphitic layers contacting an intercalated species (bounding layers) is distinguished from that of other graphitic layers without any contact with the intercalated species (interior layers) [28]. The relative Raman intensity varies depending on the ratio of bounding layers to interior layers, i.e. the stage number [28]. Thus, Raman spectroscopy gives direct insight into charge transfer behavior as a function of stage number. Some Raman spectroscopic studies have been performed to characterize C_xF samples [14,29,30]. Mallouk et al. [14] reported Raman spectroscopic data for stage 1 $C_xF_{1-\delta}(HF)_\delta$ ($2 \leq x \leq 5$). Rao et al.

* Corresponding author. Tel.: +81-565-48-8121; fax: +81-565-48-0076.
E-mail address: nakajima@ac.aitech.ac.jp (T. Nakajima).

0022-1139/01/$ – see front matter
PII: S0022-1139(01)00422-5

Table 1
X-ray diffraction data and compositions of C_xF samples prepared with K_2NiF_6 or $KAgF_4$ and elemental fluorine at room temperature

Sample[a]	F_2 ($\times 10^5$ Pa)	Fluoride	X-ray diffraction data			Composition
			Stage[b]	I_c (nm)	a_0 (nm)	
R-1	7.9	K_2NiF_6	1 (2) (3)	0.6435 (0.9334) (1.231)	0.2464	$C_{1.88}F(HF)_{0.58}$
R-2	11.8	K_2NiF_6	1	0.6467	0.2466	$C_{1.64}F$
R-3	11.8	K_2NiF_6	1 (2) (3)	0.6388 (0.9418) (1.240)	0.2466	$C_{1.46}F(HF)_{0.35}$
R-4	11.8	$KAgF_4$	1	0.6281	0.2477	$C_{1.37}F$
R-5	11.8	$KAgF_4$	1	0.6259	0.2473	$C_{1.25}F$

[a] Here R stands for room temperature.
[b] The figures within the parentheses indicate minor phase.

[29] also reported Raman scattering data for C_xF samples ($2.9 \leq x \leq 7.8$) prepared from vapour-grown graphite fibre. Raman spectra were also measured for $C_{12}F$ and $C_{6.4}F$ obtained from highly oriented pyrolytic graphite (HOPG) by Ohana et al. [30]. These studies showed that the E_{2g2} vibration mode appearing at 1580 cm^{-1} was initially shifted to 1615 cm^{-1} by fluorine intercalation into graphite in the same manner as that for other acceptor type GICs [29]. As the composition of C_xF approached C_2F, a lowering of the frequencies of the Raman peak was observed [14]. This peculiar behavior is only observed for fluorine-intercalated graphite. This anomalous shift has been explained as due to a decrease in the hole concentration in the graphene layers with increasing fluorine concentration, i.e. to an increase in C–C bond length in the graphene layer, which results in a decrease in the in-plane mode frequency [29]. As mentioned above, highly fluorinated C_xF samples ($x < 2$) have recently been synthesized [27]. These C_xF samples give rise to a new interest in how the zone-center phonon frequencies behave in the region of $x < 2$ in C_xF. In this study, Raman spectra of highly fluorinated graphite samples prepared at both room and high temperatures were measured and are considered in relation to X-ray diffraction (XRD), IR and XPS studies from the viewpoints of the formation of highly fluorinated phases in graphite at room temperature, and the formation mechanism of graphite fluoride at high temperature.

2. Results and discussion

2.1. Compositions and structures of graphite samples highly fluorinated at room temperature and 515°C

K_2NiF_6 and $KAgF_4$ are highly soluble in anhydrous HF (aHF) and effectively fluorinate graphite in combination with elemental fluorine [27]. These high oxidation state fluorides are partly reduced to NiF_2 and AgF_2 during the fluorination of graphite [27]. NiF_2 and AgF_2 are practically insoluble in aHF. They are removed from the fluorinated graphite as highly soluble $Ni(AsF_6)_2$ and $Ag(AsF_6)_2$ by treating the impure product with AsF_5. The fluorination conditions, compositions and XRD data of highly fluorinated graphite samples are given in Tables 1 and 2. The samples obtained at room temperature (shown in Table 1) have high fluorine concentrations, i.e. the ratios of carbon to fluorine are in the range of 1.88–1.25, which are obviously <2. Since the small amounts of hydrogen detected in samples R-1 and R-3 are regarded as those from HF cointercalated in the graphite, the C:F ratios were calculated by subtracting the corresponding amounts of fluorine from the analytical values. No hydrogen was detected in other samples. In the samples R-1, R-2 and R-3, obtained by K_2NiF_6 and elemental fluorine, very weak diffraction lines indicating the presence of NiF_2 were observed. The samples R-4 and R-5, obtained by $KAgF_4$ and elemental fluorine, have higher fluorine contents than those prepared by K_2NiF_6. It seems that K_2NiF_6 has a stronger oxidizing capability than $KAgF_4$, destroying the carbon hexagons of graphite. As samples R-4 and R-5 contained small amounts of AgF_2 (Ag: 1–3 wt.%), the compositions of C_xF listed in Table 1 were calculated by taking into account the amounts of fluorine bonded to AgF_2. XRD data showed that the samples prepared by K_2NiF_6 and F_2 (R-1 and R-3) contained stage 2 and 3 phases as minor components, while those prepared by $KAgF_4$ and F_2 (R-4 and R-5) were pure stage 1

Table 2
Compositions of C_xF samples prepared with elemental fluorine at 515°C

Sample[a]	Fluorination time (min)	Composition	Color
H-1	1	$C_{1.90}F$	Black
H-2	2	$C_{1.45}F$	Black-brown
H-3	3	$C_{1.27}F$	Brown
H-4	15	$C_{1.21}F$	Gray-brown
H-5	30	$C_{1.19}F$	Gray
H-6	600	$C_{1.06}F$	White

[a] Here H stands for high temperature.

compounds. The repeating distances along the c-axis (I_c values) of all the samples in Table 1 are slightly larger than 0.6 nm, suggesting that intercalated fluorine atoms make a double row between two graphene layers. The lattice parameters along the a-axis (a_0 values) are also larger than those of graphite, 0.2461 nm, meaning that the samples or their major components are highly fluorinated stage 1 compounds [4]. The C–F bonding is ionic or nearly ionic for C_xF of stage ≥ 2. However, intercalated fluorine atoms are covalently bonded to the carbon atoms of planar graphene layers for C_xF of stage 1 (semi-ionic or semi-covalent C–F bonds) [3,4,11–15]. When the ionic bond is dominant in C_xF (stage ≥ 2), the C–C bond length of the graphene layer, i.e. the a_0 value, is shortened by electron transfer from graphite to intercalated fluorine in a similar manner as in the case of the usual acceptor type graphite intercalation compounds [4]. At stage 1, the a_0 value gradually increases with increase in the number of intercalated fluorine atoms, approaching 0.2480 nm, which is larger than the value of 0.2461 nm of graphite itself. The a_0 values in Table 1 coincide with those previously reported [11,13–15].

C_xF samples prepared at 515°C were also highly fluorinated to $x < 2$ in C_xF, as shown in Table 2. The color of the samples changed from black to white with increasing time of fluorination and consequently higher fluorine content. The samples fluorinated for 1–3 min (H-1, H-2 and H-3) were black to brown, while those fluorinated for 15 min or more were gray-brown to white, suggesting that these samples (H-4, H-5 and H-6) are graphite fluorides with puckered graphene layers [3,26]. XRD measurements indicated that sample H-1 contained unreacted graphite, showing (0 0 2) and (0 0 4) lines of graphite, while sample H-2 possessed a very weak (0 0 2) line. All other samples were completely fluorinated. No (0 0 1) diffraction lines of graphite fluoride were observed for any of the samples, probably because the original graphite with a layered structure was a fine powder with an average particle diameter of 7 μm, and therefore fluorinated samples are easily disordered along the c-axis. On the other hand, (1 0 0) lines were observed for all the samples.

Fig. 1 shows typical C_{1s} and F_{1s} photoelectron spectra of graphite samples fluorinated at room temperature and 515°C. XPS analyses only a thin surface region of a solid sample (the detection depth is usually only several nm). Sample R-5 prepared at room temperature has two C_{1s} peaks at 290.4 and 287.7 eV indicating carbon atoms bound and unbound to fluorine, and also an F_{1s} peak at 688.7 eV with a low intensity peak at 686.7 eV. The binding energies of C_{1s} and F_{1s} electrons, 290.4 and 688.7 eV, suggest that the main C–F bond is semi-ionic because some charging effect may be included in such a highly fluorinated graphite sample [31,32]. The weak peak at 686.7 eV would indicate the presence of a nearly ionic C–F bond. Other samples prepared at room temperature exhibited similar spectra to those of sample R-5. NiF_2 and AgF_2 were not detected, probably because they were enclosed in graphene layers. The surface

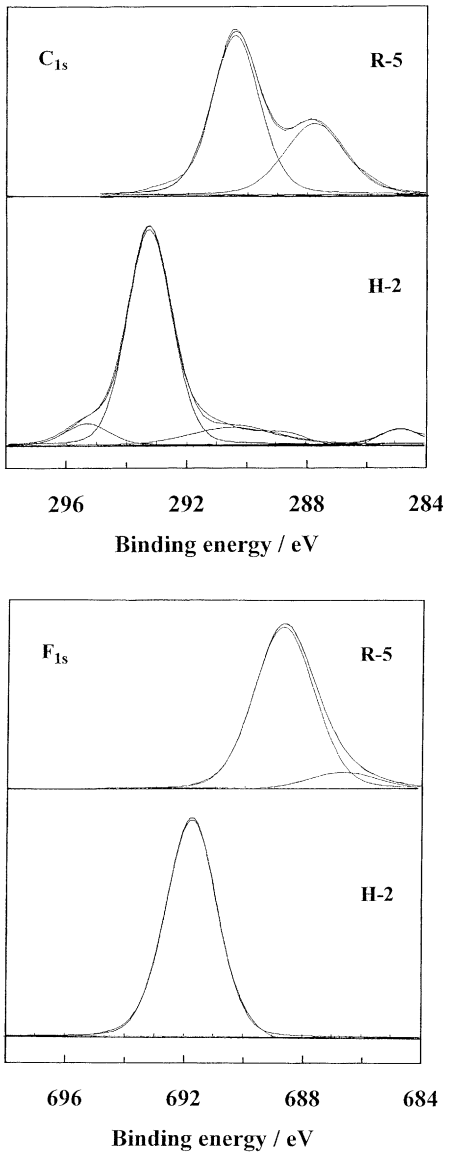

Fig. 1. C_{1s} and F_{1s} photoelectron spectra of highly fluorinated graphite samples (R-5 and H-2 in Tables 1 and 2).

of sample H-2 prepared at 515°C is more strongly fluorinated, i.e. the main C_{1s} and F_{1s} peaks are shifted to 293.2 and 691.7 eV, respectively, due to the charging effect. These binding energies are evidence for covalent C–F bonds [32,33]. Among five samples prepared at 515°C, only H-1 fluorinated for 1 min contained small amounts of semi-ionic C–F bonds and unreacted graphite. Thus, the C–F bonds of the sample surfaces are different, depending on the fluorination temperatures.

The depth of solid material analyzed is deeper in the case of IR absorption spectroscopy than XPS. Fig. 2 shows typical IR absorption spectra. Other samples have similar spectra to those shown in Fig. 2. Sample R-5 obtained at room temperature clearly shows a strong absorption, indicating the stretching vibration of a semi-ionic C–F bond at 1134 cm^{-1} with a weak intermediate absorption at

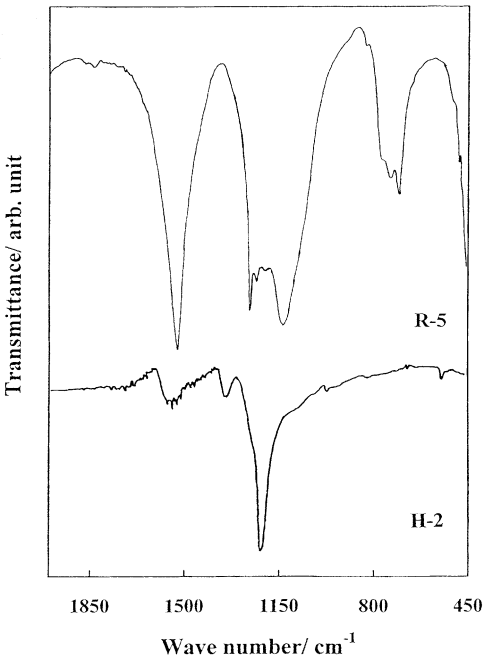

Fig. 2. IR absorption spectra of highly fluorinated graphite samples (R-5 and H-2 in Tables 1 and 2).

1196 cm^{-1}, a weak absorption by a covalent C–F bond at 1231 cm^{-1} and another absorption at 1256 cm^{-1} [14,33]. The absorption due to the semi-ionic C–F bonds varied from 1125 to 1134 cm^{-1} with increasing duration of fluorination. These data show that the vibration energies of semi-ionic C–F bonds of samples R-1–R-5 are slightly stronger than that observed for C_2F (1100 cm^{-1}) [14]. The absorption at 1196 cm^{-1} suggests the existence of a more highly fluorinated C_xF phase such as C_1F because the peak position is close to that of a covalent C–F bond. The strong absorption at 1522 cm^{-1} is due to the A_{2u} vibration mode of the graphite lattice [34]. This absorption is located at a low frequency because of the decrease in vibrational energy arising from the increase in C–C bond length at a high degree of fluorination (see a_0 values in Table 1). On the other hand, sample H-2 obtained at 515°C shows the existence of a strongly fluorinated graphite phase with covalent C–F bonds. The strong absorption at 1218 cm^{-1} is very close to that due to the stretching vibration of a tertiary C–F bond, and the weak absorption at 1341 cm^{-1} is assigned to asymmetric stretching vibrations of peripheral CF_2 groups [33]. A broad absorption is also observed at 1542 cm^{-1}, which indicates that a fluorinated graphite phase with planar graphene layers exists in sample H-2. This absorption was weakened with increasing duration of fluorination and completely disappeared in sample H-5.

2.2. Raman spectra of highly fluorinated graphite samples

Figs. 3 and 4 show Raman spectra of graphite powder and graphite samples fluorinated at room temperature and

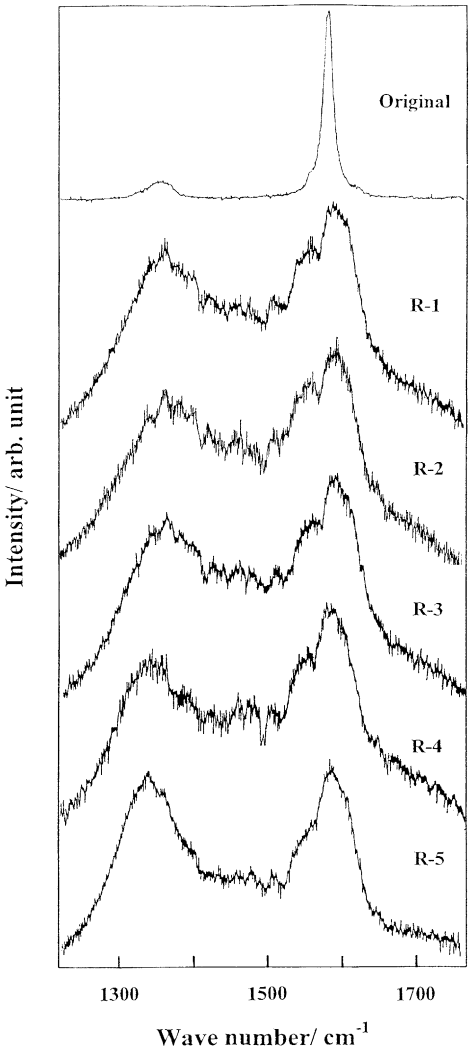

Fig. 3. Raman spectra of original graphite and samples fluorinated at room temperature (sample numbers are given in Table 1).

515°C. Graphite powder has two Raman bands at 1580 and 1360 cm^{-1}. The band with high intensity observed at 1580 cm^{-1} is from an E_{2g2} vibration mode of the graphene layers (G-band), and that at 1360 cm^{-1} is due to an A_{1g} mode usually observed for powdery graphite having a large area of edge planes or carbon materials with low crystallinity (D-band) [35,36]. Highly fluorinated C_xF samples prepared at room temperature exhibited strong G-bands at 1593–1583 cm^{-1} with lower frequency bands at 1555–1542 cm^{-1}, and D-bands at 1356–1337 cm^{-1} as shown in Fig. 3. The D-band intensity was also significantly enhanced by fluorination, suggesting high disorder of the C_xF samples. The peak positions of the three Raman bands shifted to lower frequencies with increasing fluorine content in C_xF, i.e. from 1593, 1555 and 1356 cm^{-1} to 1583, 1542 and 1337 cm^{-1}, respectively. This means that the vibrational energy of graphene layers decreases with increase in the fluorine content of C_xF. The decrease in vibrational energy is due to a weakening of the C–C bond [29], i.e. an increase in the

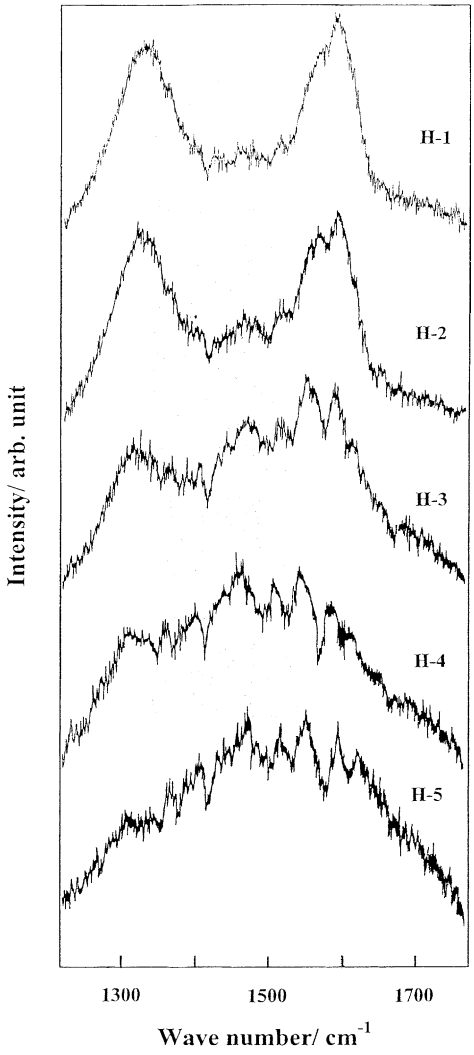

Fig. 4. Raman spectra of graphite samples fluorinated at 515°C (sample numbers are given in Table 2).

C–C bond length with increase in fluorine content, as given in Table 1. The frequency of the G-band moved to the original position, 1580 cm^{-1}, as the composition of C_xF approached C_2F [14]. Plots of Raman frequencies for the main peaks are given in Fig. 5, which includes previously published data [14,29,30]. In the region of fluorine concentrations higher than C_2F, the low frequency G-bands are divided into two groups. The new bands observed at 1555–1542 cm^{-1} suggest the formation of a more highly fluorinated phase, C_1F. The existence of two groups in the plots suggests the coexistence of two highly fluorinated phases such as C_2F and C_1F. Possible structures of highly fluorinated graphite are C_2F and C_1F. A structural model of C_2F was reported before [14]. In C_1F, fluorine atoms are bonded above and below to all the carbon atoms of planar graphene layers. C_xF samples prepared at room temperature may be a mixture of two fluorinated phases, C_2F and C_1F. This is consistent with the fact that the composition of C_xF is between C_1F and C_2F, as given in Table 1. D-bands have

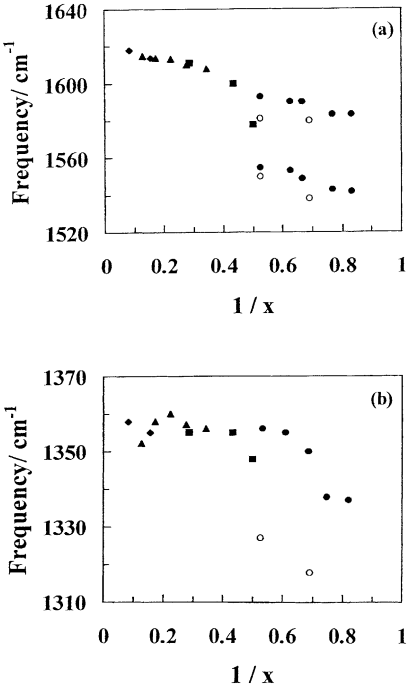

Fig. 5. Raman shifts as a function of $1/x$ in C_xF. (■): [14], (▲): [29], (◆): [30], (●): this work (obtained at room temperature), (○): this work (obtained at 515°C).

the similar trend to shift to lower frequency with increase in fluorine concentration.

It is surprising that Raman spectra with the same profile as those for C_xF samples prepared at room temperature have been obtained for graphite samples fluorinated at 515°C for 1 and 2 min as shown in Fig. 4. The peak frequencies plotted in Fig. 5 are consistent with the data obtained for the samples prepared at room temperature. The frequency reduction is larger, in particular in the D-bands because samples H-1–H-5 are more strongly fluorinated at 515°C. The profile of the Raman spectrum of sample H-3 obtained by 3 min fluorination is somewhat changed. Samples fluorinated for 15 min to 10 h no longer exhibited the kind of profiles seen for C_xF samples, which means that samples H-4 and H-5 are completely changed to graphite fluoride with puckered graphene layers. The spectra of samples H-4 and H-5 in Fig. 4 were highly magnified because they were recorded with high sensitivity. The color change of the samples correlates with the change in the profile of the Raman spectra. C_xF samples prepared at room temperature are all black; however, those prepared at 515°C are black, or brown to white depending on the duration of fluorination. The samples H-4 and H-5 with gray-brown and gray colors have lost the original profile of the Raman spectra. The change of the Raman spectrum profile with time of fluorination corresponds to the change of the sp^2 to sp^3 hybridization of the carbon orbitals of fluorinated graphite accompanying the color change, that is, the planar graphene layer is changed to a cyclohexane chair. This change in the graphene layers is shown by the formation of graphite fluoride as an electric insulator, in which the

electrons are strongly localized and the band gap is larger than 3 eV. The details of the process of formation of graphite fluoride by high temperature fluorination were unknown to date. The Raman spectra shown in Fig. 4 reveal the stages of fluorination of graphite at high temperature. Fluorine atoms are intercalated into the graphene layers, forming a fluorine-intercalated phase which is similar to highly fluorinated C_xF prepared at room temperature. At this stage, the graphene layers keep their planarity; however, the C_xF phase with planar graphene layers is quickly changed to graphite fluoride having puckered graphene layers, probably with accompanying partial carbon–carbon bond breaking. Thus, Raman spectroscopy is a good tool for detecting the change of sp^2 to sp^3 hybridization of carbon orbitals in fluorinated graphite.

3. Conclusion

This Raman study of highly fluorinated graphite samples revealed that C_xF samples ($1 < x < 2$) prepared both at room temperature and 515°C (fluorination for 1 and 2 min at 515°C) give two Raman bands suggesting the coexistence of C_2F and C_1F phases with planar graphene layers. The Raman bands are shifted to lower frequencies with increasing fluorine concentration and *a*-axis lattice parameter of C_xF.

The formation mechanism of graphite fluoride at high temperature was clarified by Raman spectroscopy for graphite samples fluorinated in the time range of 1 min to 10 h at 515°C. In the initial stages of fluorination of graphite by elemental fluorine, fluorine is intercalated into the surface region of the graphite to form a C_xF phase with planar graphene layers. The C_xF phase is quickly changed to graphite fluoride with puckered graphene layers when fluorination at higher temperature (515°C) and longer times (more than 3 min) was performed.

4. Experimental

4.1. Synthesis of highly fluorinated graphite samples at room temperature and 515°C

For the preparation of highly fluorinated graphite samples at room temperature, natural graphite powder (particle size: 57–74 μm, purity: 99.4%) was fluorinated by K_2NiF_6 (Ozark Mahoning, Pennwalt, purity: 99.5%) or $KAgF_4$ [37] and elemental fluorine under pressure (Solvay, purity: 99%, $(7.9–11.8) \times 10^5$ Pa) in anhydrous HF (aHF, Praxair, purity: 99.9%). The prepared C_xF samples were contaminated with by-products insoluble in aHF, either NiF_2 or AgF_2. To remove these impurities the prepared C_xF samples were treated by AsF_5 in order to obtain products very soluble in aHF, $Ni(AsF_6)_2$ or $Ag(AsF_6)_2$. Anhydrous HF used as a solvent in the above reactions was treated with K_2NiF_6 for several days prior to use, and $KAgF_4$ was prepared as described elsewhere [37]. AsF_5 was prepared as described for the synthesis of PF_5 [38]. The details of the experimental procedure are described in a previous paper [27].

Fluorination of graphite powder (average diameter: 7 μm) was performed at 515°C by elemental fluorine (1×10^5 Pa, Daikin Industries, Ltd., purity: 99.4–99.7%) for different fluorination times in the range from 1 min to 10 h in a batch-type nickel reactor.

4.2. Analyses of the products

The fluorinated graphite samples were analyzed for carbon, hydrogen and fluorine at the Elemental Analysis Center of the Faculty of Pharmaceutical Science of Kyoto University. Raman spectroscopy (Jobin–Yvon T-64000 with Ar ion laser of 514.5 nm), X-ray photoelectron spectroscopy (XPS, Ulvac Phi Model 5500 with Mg Kα radiation), IR absorption spectroscopy (Perkin-Elmer 2000, KBr disk method) and X-ray diffractometry (Shimadzu XD-610 with Cu Kα radiation) instrumental methods were used for characterization of the fluorinated graphite samples. The small amounts of silver contained in samples R-4 and R-5 in Table 1 were analyzed at the Jozef Stefan Institute as follows. The sample was hydrolyzed in HNO_3 solution and heated on a sand bath for 2 h with further addition of HNO_3. After filtration, the amount of silver in the filtrate was determined by atomic absorption spectroscopy. The amount of silver in the solid residue was also obtained by atomic absorption spectroscopy after decomposition of the solid residue in a melt of $KNaCO_3$. The binding energies of XPS peaks were determined relative to that of the C_{1s} electron of graphite at 284.3 eV without a charging correction.

References

[1] W. Rüdorff, G. Rüdorff, Chem. Ber. 80 (1947) 417–423.
[2] R.J. Lagow, R.B. Badachhape, P. Ficalora, J.L. Wood, J.L. Margrave, Synth. Inorg. Metal-Org. Chem. 2 (1972) 145–149.
[3] T. Nakajima, N. Watanabe, Graphite Fluorides and Carbon–Fluorine Compounds, CRC Press, Boca Raton, FL, 1991.
[4] T. Nakajima, in: T. Nakajima (Ed.), Fluorine–Carbon and Fluoride–Carbon Materials: Chemistry, Physics and Applications, Marcel Dekker, New York, 1995, pp. 1–31.
[5] T. Nakajima, M. Kawaguchi, N. Watanabe, Z. Naturforsch. 36b (1981) 1419–1423.
[6] T. Nakajima, M. Kawaguchi, N. Watanabe, Carbon 20 (1982) 287–291.
[7] T. Nakajima, M. Kawaguchi, N. Watanabe, Synth. Metals 7 (1983) 117–124.
[8] T. Nakajima, N. Watanabe, I. Kameda, M. Endo, Carbon 24 (1986) 343–351.
[9] T. Nakajima, T. Ino, N. Watanabe, H. Takenaka, Carbon 26 (1988) 397–401.
[10] T. Nakajima, M. Molinier, M. Motoyama, Carbon 29 (1991) 429–437.
[11] T. Nakajima, M. Namba, Tanso 170 (1995) 255–258.
[12] T. Nakajima, Y. Matsuo, B. Žemva, K. Lutar, Carbon 34 (1996) 1595–1598.

[13] T. Mallouk, N. Bartlett, J. Chem. Soc., Chem. Commun. (1983) 103–104.
[14] T. Mallouk, B.L. Hawkins, M.P. Conrad, K. Zilm, G.E. Maciel, N. Bartlett, Phil. Trans. R. Soc. London Ser. A 314 (1985) 179–187.
[15] R. Hagiwara, M. Lerner, N. Bartlett, J. Chem. Soc., Chem. Commun. (1989) 573–574.
[16] I. Palchan, D. Davidov, H. Selig, J. Chem. Soc., Chem. Commun. (1983) 657–658.
[17] I. Palchan, D. Davidov, V. Zevin, G. Polatsek, H. Selig, Synth. Metals 12 (1985) 413–418.
[18] A. Hamwi, M. Daoud, J.C. Cousseins, Synth. Metals 26 (1988) 89–98.
[19] T. Nakajima, M. Kawaguchi, N. Watanabe, Solid State Ionics 11 (1983) 65–69.
[20] T. Nakajima, B. Chang, T. Fujiwara, N. Watanabe, M. Endo, Carbon 26 (1988) 213–215.
[21] D. Vaknin, I. Palchan, D. Davidov, H. Selig, D. Moses, Synth. Metals 16 (1986) 349–365.
[22] I. Ohana, I. Palchan, Y. Yacoby, D. Davidov, H. Selig, Phys. Rev. B 38 (1988) 12627–12632.
[23] H. Touhara, Y. Goto, N. Watanabe, K. Imaeda, T. Enoki, H. Inokuchi, Y. Mizutani, Synth. Metals 23 (1988) 461–466.
[24] L. Piraux, V. Bayot, J.P. Issi, M.S. Dresselhaus, M. Endo, T. Nakajima, Phys. Rev. B 41 (1990) 4961–4969.
[25] A. Tressaud, V. Gupta, L. Piraux, L. Lozano, E. Marquestaut, S. Flandrois, A. Marchand, O.P. Bahl, Carbon 32 (1994) 1485–1492.
[26] N. Watanabe, T. Nakajima, H. Touhara, Graphite Fluorides, Elsevier, Amsterdam, 1988.
[27] T. Nakajima, M. Koh, V. Gupta, B. Žemva, K. Lutar, Electrochim. Acta 45 (2000) 1655–1661.
[28] M.S. Dresselhaus, G. Dresselhaus, Adv. Phys. 30 (1981) 139–326.
[29] A.M. Rao, A.W.P. Fung, S.L. di Vittorio, M.S. Dresselhaus, G. Dresselhaus, M. Endo, K. Oshida, T. Nakajima, Phys. Rev. B 45 (1992) 6883–6891.
[30] I. Ohana, I. Palchan, Y. Yacoby, D. Davidov, H. Selig, Solid State Commun. 56 (1985) 505–508.
[31] Y. Matsuo, T. Nakajima, Z. Anorg. Allg. Chem. 621 (1995) 1943–1950.
[32] Y. Matsuo, T. Nakajima, S. Kasamatsu, J. Fluorine Chem. 78 (1996) 7–13.
[33] Y. Kita, N. Watanabe, Y. Fujii, J. Am. Chem. Soc. 101 (1979) 3832–3841.
[34] R.J. Nemanich, G. Lucovsky, S.A. Solin, Solid State Commun. 23 (1977) 417–420.
[35] F. Tuinstra, J.L. Koenig, J. Chem. Phys. 53 (1970) 1126–1130.
[36] D.S. Knight, W.B. White, J. Mater. Res. 4 (1989) 385–393.
[37] K. Lutar, S. Milicev, B. Žemva, B.G. Muller, B. Bachmann, R. Hoppe, Eur. J. Solid State Inorg. Chem. 28 (1991) 1335–1346.
[38] A. Jesih, B. Žemva, Vest. Slov. Kem. Drus. 33 (1986) 25–28.